



ELSEVIER

1 April 2002

Optics Communications 204 (2002) 311–315

OPTICS
COMMUNICATIONS

www.elsevier.com/locate/optcom

Single frequency, continuously tunable, diode-pumped Nd:LiY_{0.5}Gd_{0.5}F₄ microlaser

N.U. Wetter*, P.S.F. de Matos, I.M. Ranieri, L.C. Courrol, S.P. Morato

*Centro de Lasers e Aplicações, Instituto de Pesquisas Energéticas e Nucleares, IPEN/SP, R. Travessa R 400,
Cidade Universitária, 05508-900 São Paulo S, Brazil*

Received 8 October 2001; received in revised form 1 February 2002; accepted 7 February 2002

Abstract

We have studied the single frequency lasing performance of a neodymium doped microlaser that uses the new host material LiY_{0.5}Gd_{0.5}F₄. Using a very compact cavity design and combining techniques of hole burning mode suppression and frequency selection we achieve a smoothly tunable bandwidth of more than 150 GHz. In a high brightness, longitudinal diode-pumped set-up we obtain 200 mW of continuous single frequency output power. © 2002 Elsevier Science B.V. All rights reserved.

Single frequency, compact and efficient diode-pumped solid-state lasers are nowadays commonly used for innumerable industrial and scientific applications. They are of special interest for all kinds of non-linear optical frequency conversion [1] and for use in atmospheric DIAL measurements [2]. In these cases, their output should be stable, have narrow linewidth and, if possible, be tunable. Microchip lasers are monolithic solid-state lasers with a cavity length typically of the order of a millimeter, well suited for single frequency, single mode operation [3,4]. For single frequency operation their cavity mode spacing has to be larger than the gain bandwidth. This generally limits the cavity to a very short length. Therefore, these lasers are

limited in output power, have relatively large linewidth and are not tunable without some degree of mode hopping. Larger microchip lasers of higher output power, which operate single frequency, have been built [3] mostly for q-switched operation. Microlasers have larger cavities (of the order of one centimeter) permit higher output power, smaller linewidth and can easily incorporate better tuning techniques but need additional mode selection devices, which tend to introduce losses [5,6].

We use a set of coupled cavities whose main cavity's mode spacing is smaller than the gain bandwidth but still large enough to achieve suppression of all but one spectral hole burning mode (SHB), using additional mode selecting techniques. The set-up is very compact and does not need specially coated crystal surfaces as required by microchip lasers with the gain medium at the end of the cavity. For diode-pumping and frequency tuning purposes, Nd:LiY_{0.5}Gd_{0.5}F (Nd:GYLF)

*Corresponding author. Tel.: +55-113816-9305; fax: +55-113816-9315.

E-mail address: nuwetter@net.ipen.br (N.U. Wetter).

crystals are of advantage when compared to Nd:YAG or Nd:YLF. They present the same spectroscopic parameters as Nd:YLF but have a larger bandwidth (1.6 nm) and a higher segregation coefficient, which permits higher neodymium doping levels [7].

Single frequency oscillation in standing wave cavities with homogeneously broadened gain media is hampered by spectral hole burning (SHB) [8]. It has been shown that the separation of the hole burning modes, $\Delta\nu$, for a laser media, which is in contact with one of the resonator mirrors, is given by multiples of

$$\Delta\nu = \frac{c}{2nl}, \quad (1)$$

where c is the speed of light, n and l are the refractive index and the crystal's length, respectively [9]. In the case of a very thin active media, which is not attached to one of the resonator mirrors, the hole burning mode separation can be approximated by

$$\Delta\nu = \frac{c}{4d}, \quad (2)$$

where d is the distance between the nearest resonator mirror and the crystal face [10]. For the general case of a gain media that is long compared to the cavity length and which is not in contact with one of the mirrors, the SHB mode separation can be easily deduced, as will be shown next.

Generally, the first longitudinal mode to oscillate inside the resonator is the one closest to the gain peak. This mode establishes a standing wave pattern whose steady-state inversion is “burned” into the gain media. The second mode to start

oscillation is the one which best exploits the remaining, not depleted inversion. It can be shown [11,12] that this second mode is in phase with the not depleted inversion exactly in the middle of the gain medium. This is also easily understood, because only by fulfilling this condition for the second mode frequency, the maximums of its intensity pattern stay in phase over the longest possible distance with the maximums of the not depleted inversion. This generates the largest possible overlap integral of inversion and intensity, resulting therefore in maximum gain for the second mode. It follows that the two modes are 90° out of phase exactly in the middle of the gain media. Therefore, the separation of the hole burning modes, $\Delta\nu$, for a laser media, which is not in contact with one of the resonator mirrors, is given by

$$\Delta\nu_{\text{SHB}} = \frac{c}{2(nl + 2d)}. \quad (3)$$

By making the overall cavity length just a little bit bigger than $(nl + 2d)$, the cavity mode separation is smaller than $\Delta\nu_{\text{SHB}}$. Depending upon the gain and the cavity mode separation, the frequency difference between two hole burning modes that actually oscillate, can be a multiple of $\Delta\nu_{\text{SHB}}$. Fine-tuning of the difference between cavity mode separation and $\Delta\nu_{\text{SHB}}$ and of the available gain permits therefore to suppress several adjacent hole burning modes. Additionally, the cavity set-up permits not only changes in the cavity length, ΔL , but also changes of the crystal position, Δd (see Fig. 1). Therefore, the hole burning mode frequency can be adjusted continuously.

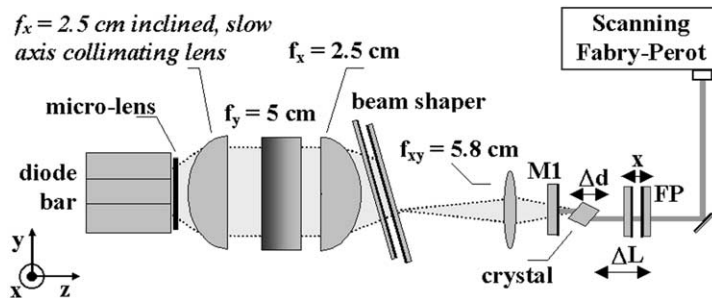


Fig. 1. Optical arrangement of the pump set-up and the microlaser. The laser cavity is formed by the curved mirror M1 and the coupled Fabry-Perot cavity (FP).

The single crystal was grown by the Czochralski technique under high purity argon or CF_4 atmosphere. GdF_3 , YF_3 , NdF_3 and LiF pure commercial powders (Rare Metallic 99.99%), were added in the crucible and melted in CF_4 (99.9999%) atmosphere prior to the growth. The crystal-pulling rate was 0.6 mm/h for a $\langle 100 \rangle$ -oriented boule, with 8 rpm rotation rate. The Nd:GYLF crystal, with a composition in the melt of 66 mol% LiF and 34 mol% $\text{Gd}_{0.5}\text{Y}_{0.473}\text{Nd}_{0.027}\text{F}_3$, was grown maintaining CF_4 atmosphere. A crystal of good quality was obtained, with fine planes of micro defects near the seed that disappeared as the diameter increased. The crystal was free of scattering centers under inspection with a He–Ne laser. The co-doping with yttrium is an important advantage, when compared to Nd:GLF crystals, because it apparently decreases the liquid viscosity, making the convective flow in the melt appropriate to the diffusion of the major component that is LiF and neodymium. As a result, excellent quality crystals can be obtained.

The 792 nm, 20 W diode bar used in this experiment (Opto Power) has a total width of 1 cm which comprises of 24 emitters, each measuring $1 \times 200 \mu\text{m}^2$ (height \times width), with center to center spacing of 400 μm . The emitted beam is collimated in the fast direction (x -axis) by a factory installed, AR-coated non-cylindrical fiber lens of 440 μm diameter, as shown in Fig. 1. A two-mirror beam-shaper [13] was used, to reconfigure the diode emission into a more circular beam with approximately equal M^2 factors in the x - and y -direction. A significant amount of diode array curvature was detected, causing a severe power loss during the reshaping procedure of the diode emission. The array curvature was partially compensated by using the procedure described in [14]. The final beam quality at the crystal position was $M^2 = 45$ in the x -direction and $M^2 = 30$ in the y -direction, as measured with a CCD camera (Merchantek model WinCam), and the maximum obtainable power was 16.1 W.

The laser cavity comprises mirror M1 (see Fig. 1), the Nd:GYLF gain media and a coupled Fabry–Perot cavity, which forms the output coupler. The input mirror M1 was curved (radius of curvature of 30 cm), had a highly reflective coating for

the lasing wavelength ($R > 99\%$) and a high transmission ($T = 95\%$) for the pump wavelength. The length of the Brewster-cut laser crystal was 2.9 mm. This smaller crystal length was necessary in order to achieve a larger separation between adjacent hole burning modes. Due to this reduced length the crystal did not absorb all pump radiation. The z -axis position of the crystal could be adjusted with a differential micrometer screw to determine roughly the hole burning modes. The pump beam waist at the crystal position was 180 μm using a focusing lens of $f = 58$ mm. This small beam waist is a direct consequence of the good pump beam quality. The pump beam waist is slightly larger than the calculated intracavity mode, which experimentally gave the best results. Using a flat output coupler with 88% reflectivity we achieved with this crystal 3.8 W of output power at 15 W of incident pump power and 320 mW at 2.8 W of input power. This latter data is important for comparison with the laser's performance at single frequency. The overall cavity length was 12 mm and the crystal input face had a distance of 2 mm from the input mirror due to its shape cut at Brewster angle.

For the single frequency operation we replaced the flat output coupler by a coupled cavity with two flat mirrors of 70% and 48% reflectivity, forming a Fabry–Perot. The intermediate mirror's surface without coating faced the crystal. The distance, x , between both mirrors, could be changed interferometrically with a differential micrometer. Additionally, the coupled cavity was on top of a z -axis translation stage whose position was controlled by a piezorestrictive actuator permitting changes, ΔL , in the main cavity length (see Fig. 1). The Fabry–Perot (FP) coupled cavity serves at the same time as output coupler and as selector of the oscillating wavelength. It restricts the number of oscillating SHB modes by periodically modulating the spectral reflectivity profile, introducing losses at the reflection minima. The interferometrically controlled FP cavity length and the reflectivity of the mirror coatings determine the spectral width of the reflection minima and the maximum value of the reflectivity, respectively. In order to achieve a strong mode selectivity, which discriminates against unwanted SHB modes, the

maximum reflectivity of the FP cavity was chosen to be close to the lasers optimum reflectivity that was previously measured experimentally. Therefore, resonator loss is immediately increased for an oscillating frequency once the FP cavity is detuned from the peak reflectivity. Because the FP is used at anti-resonance there is only one set of cavity modes that may oscillate, determined solely by the main cavity length. This further increases the mode selectivity as opposed to FP cavities that use a high reflectivity mirror at the end and a low reflectivity mirror close to the gain media, which is known to generate two sets of cavity modes [15]. The effective reflectivity returned by the coupled cavity is easily calculated

$$R_{\text{eff}} = \frac{R_1 + R_2 - 2\sqrt{R_1 R_2} \cos(\Theta)}{1 + R_1 R_2 - 2\sqrt{R_1 R_2} \cos(\Theta)}, \quad (4)$$

where R_1 and R_2 are the reflectivities of the two mirrors that compose the empty cavity and $\Theta = 4\pi x/\lambda$, x being the mirror separation (as shown in Fig. 1). The frequency spectrum was analyzed with a fiber coupled, mode-matched, scanning FP (Burleigh Instruments, model HIF-ASE) and recorded with a digital oscilloscope (Tektronix, model TDS 360). The oscilloscope readout was calibrated using the procedure of the scanning FP's manual that is based on the measured interval between the higher order etalon modes divided by the measured free spectral range. This assures accurate calibration even if the distance between the mirrors is less than one millimeter.

By lowering the pump power until 1.6 W we achieved 27 mW of single frequency output power using a single mirror, 88% reflectivity output coupler. Using the coupled cavity as the output coupler and 2.8 W of pump power, the frequency of the output could be continuously tuned, although there were generally two to three hole burning modes oscillating at the same time. To tune to the desired emission frequency we adjusted the distance, x , between the FP mirrors. Fine-tuning of the strongest SHB mode was achieved by changing the crystal position, Δd , with the attached differential micrometer. Finally, in order to suppress the additional SHB modes, the main cavity length was changed by ΔL until all modes

disappeared except one, as shown in Fig. 2. Changing both parameters, ΔL and Δd , permits tuning of any frequency within the tuning range without the typical mode hopping. This is especially of advantage if a specific frequency has to be selected. By repeating this procedure and changing the FP's overall cavity length by approximately half a micron we achieved the tuning curve of Fig. 3. Altogether, the set-up uses a total of four mode selecting techniques in a very compact form. These are: frequency selection (change of crystal position) and enhancement (interferometric adjustment of x and selection of suitable mirror reflectivities), hole burning mode suppression (adjustment of main cavity length) and bandwidth limitation (rough adjustment of x).

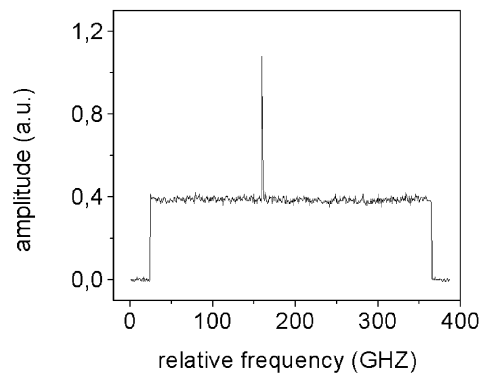


Fig. 2. Single frequency scan obtained at 2.8 W of pump power.

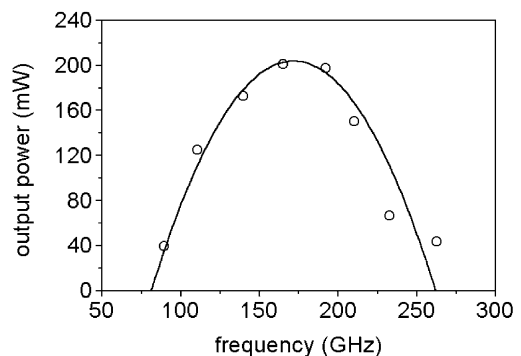


Fig. 3. Single frequency tuning curve of the Nd:GYLF laser. The solid line is a guide to the eye.

Using a coupled cavity length of approximately 1 mm we achieved a maximum output power of 200 mW at 2.8 W of input power at the center of the tuning range of more than 150 GHz (see Fig. 3). This value is close to the 320 mW multi-mode output achieved with the 88% reflector, reminding that we have additional losses due to the non-anti-reflection coated intermediate mirror of the coupled cavity. Increase in the pump power above 2.8 W always resulted in multi-mode operation independently of the coupled cavity's length. Using bigger and more complex coupled cavity designs [16], it should be possible to achieve better mode selectivity, which in turn permits the use of even higher pump powers obtaining larger tuning ranges and higher output powers. The mechanical stability of the set-up permitted oscillation of a specific single frequency for more than 5 min. After that, the main cavity length had to be readjusted electronically so that the same mode could continue to oscillate. The resolvable bandwidth was limited by the scanning FP to 150 MHz.

In conclusion, we carried out experiments on the lasing performance of a Nd:GYLF laser with a coupled cavity. The host material GYLF proved suitable for tunable, single frequency operation, allowing for high power (200 mW) output and large tunable bandwidth (150 GHz). Due to the tuning and hole burning mode suppression mechanism used in our experiment, fine-tuning of any desired frequency within the overall tuning range can be achieved.

Acknowledgements

The authors would like to thank the support of FAPESP, Fundação de Amparo à Pesquisa do Estado de São Paulo, grant no. 95/9503-5.

References

- [1] C. Pedersen, P.L. Hansen, P. Buchhave, T. Skettrup, *J. Appl. Opt.* 36 (1997) 6780.
- [2] U.N. Singh, J. Yu, in: *Advances in Laser Remote Sensing, Selected Papers Presented at the 20th International Laser Radar Conference*, 2000, p. 45.
- [3] E. Molva, *Opt. Mater.* 11 (1999) 289.
- [4] J.J. Zayhowski, *Opt. Mater.* 11 (1999) 255.
- [5] P. Laporta, S. Taccheo, S. Longhi, O. Svelto, C. Svelto, *Opt. Mater.* 11 (1999) 269.
- [6] J. Izawa, H. Nakajima, H. Hara, Y. Arimoto, *Opt. Commun.* 180 (2000) 137.
- [7] I.M. Ranieri, K. Shimamura, K. Nakono, T. Fujita, L.C. Courrol, S.P. Morato, T. Fukuda, *J. Crystal Growth* 217 (2000) 145.
- [8] C.L. Tang, H. Statz, G. deMars, *J. Appl. Phys.* 34 (1963) 2289.
- [9] J.J. Zayhowski, *Opt. Lett.* 15 (1990) 431.
- [10] N.D. Vieira Jr., L.F. Mollenauer, *IEEE J. Quantum Electron.* QE-21 (1985) 195.
- [11] F.X. Kärtner, B. Braun, U. Keller, *Appl. Phys. B* 61 (1995) 569.
- [12] B. Braun, K.J. Weingarten, F.X. Kärtner, U. Keller, *Appl. Phys. B* 61 (1995) 429.
- [13] W.A. Clarkson, D.C. Hanna, *Opt. Lett.* 21 (1996) 375.
- [14] N.U. Wetter, *Opt. Laser Technol.* 33 (2001) 181.
- [15] T. Yokozawa, J. Izawa, H. Hara, *Opt. Commun.* 145 (1998) 98.
- [16] D.J. Binks, D.K. Ko, L.A.W. Gloster, T.A. King, *Opt. Commun.* 146 (1998) 173.